JOURNAL OF CATALYSIS 122, 406–414 (1990)

Preparation and Characterization of Silica-Supported Ni/Pt Catalysts

CHRISTIAN RAAB,* JOHANNES A. LERCHER,*,[1] JAMES G. GOODWIN, JR.,† AND JOSEPH Z. SHYU‡

*Institut für Physikalische Chemie, Technische Universität Wien, Getreidemarkt 9, A-1060 Vienna, Austria; †Department of Chemical and Petroleum Engineering, University of Pittsburgh, Pittsburgh, Pennsylvania 15261; and ‡Amoco Research Center, P.O. Box 400, Naperville, Illinois 60566

Received July 6, 1989; revised November 2, 1989

The formation of a series of Ni/Pt catalysts was investigated by means of temperature-programmed reduction (TPR) of the chloride precursor, hydrogen chemisorption, X-ray diffraction, scanning electron microscopy, XPS, and magnetic measurements. An alloy between Pt and Ni was formed. The minority constituent of the series of bimetallic catalysts was always found to be quantitatively alloyed or in close contact with the more abundant metal. For several samples, the stoichiometric NiPt compound was observed. With Ni-rich samples a nonstoichiometric alloy (rich in Ni) was concluded to exist. At all concentration levels the presence of Pt facilitated the reduction of Ni^{2+} significantly. Temperature-programmed reduction of the Ni/Pt catalyst with 50 mol% and higher concentrations of Pt did not differ from that of pure Pt. Based on XPS and magnetic measurements it is concluded that a constant fraction (approximately 10–15%) of Ni was highly dispersed and interacted strongly with the support.

INTRODUCTION

Supported bimetallic catalysts offer interesting possibilities in designing the selectivity of heterogeneous catalysts and these benefits have already been exploited in several industrial processes [e.g., (*1*)]. In addition, small amounts of noble metals may be used to promote the reduction of base metals, such as nickel (*2*), and to stabilize their degree of reduction during the catalytic process.

One of the most important questions to be addressed for the characterization of supported bimetallic catalysts is whether or not alloy particles are formed. Alloy formation may occur during reduction of the catalyst precursor (usually a mixture of metal salts impregnated upon a carrier material) or (ii) during sintering of the small metal particles, formed initially by reduction of the metal salt, upon further increase of the temperature. Because the reduction step may be crucial for alloy formation, temperature-programmed reduction (TPR), as a transient response technique, is often able to provide important information on the mutual influence of the metal components (*3–5*).

In this respect, Pt/Ni bimetallic catalysts present an interesting as well as a challenging example in which both metals are important catalysts or catalyst components for industrial processes (*6–9*), showing very different catalytic behavior in the conversion of hydrocarbons and in CO hydrogenation (*10–12*).

Both Ni and Pt have fcc lattice structures and are reported to be perfectly miscible (*13*). The phase diagram shows the existence of two stoichiometric phases, NiPt and Ni_3Pt (*14*). Studies on the surface concentrations of the Ni/Pt alloy system are controversial. While some studies agree that a surface segregation of Pt exists (*13, 15–18*), others suggest that no significant surface segregation of either component takes place (*19, 20*) or that the surface layer may be enriched in Ni (*21*). Model calculations of the surface layer compositions indi-

[1] To whom correspondence should be addressed.

0021-9517/90 $3.00

cate that Ni should be preferentially present in the topmost layer (*22–24*). The enrichment in Pt observed experimentally could not be explained.

In this study we describe the genesis of a series of Ni/Pt bimetallic catalysts prepared by the incipient wetness method from chloride salts and compare the resulting materials with those of supported catalysts in earlier studies (*21, 25, 26*). Temperature-programmed reduction, hydrogen chemisorption, transmission electron microscopy, XPS, magnetic measurements, and X-ray diffraction were used as analytical means.

EXPERIMENTAL

Catalysts. A series of PtNi bimetallic catalysts were prepared using the incipient wetness technique. The composition of the samples is compiled in Table 1. The total metal loading was kept constant at 4×10^{-3} mol metal per gram of silica. The metal salts were dissolved in distilled water and subsequently mixed thoroughly with silica ($PtCl_4$, $NiCl_2 \cdot 6H_2O$ from Ventron, Aerosil 200 from Degussa). Typically, a ratio of 1.5 to 2 ml solution per gram of silica was necessary to reach incipient wetness. After the impregnation step the catalyst precursors were dried in air at temperatures between 353 and 373 K for 12 to 14 h.

TABLE 1

Metal Loading of the Samples Investigated

	Composition of the metal phase (mol%)		Metal loading (wt%)		
	Ni	Pt	Ni	Pt	Total
Ni	100	0	2.3	0.0	2.3
Ni/Pt-1	90	10	2.1	0.9	3.0
Ni/Pt-2	80	20	1.8	1.7	3.6
Ni/Pt-3	70	30	1.5	2.5	4.1
Ni/Pt-4	50	50	1.1	4.2	5.3
Ni/Pt-5	30	70	0.7	5.8	6.5
Ni/Pt-6	10	90	0.2	7.3	7.5
Pt	0	100	0	8.2	8.2

Reduction of the precursors was carried out in pure hydrogen at a flow rate of 100 ml min^{-1}, increasing the reactor temperature from ambient temperature to 773 K at 3 K min^{-1} (hydrogen from Air Liquide, 99.999 vol%, no further purification). The temperature was kept at 773 K for another 12 to 14 h before cooling to room temperature in a hydrogen atmosphere. Then H_2 was turned off and air was allowed to diffuse slowly into the reactor to passivate the catalyst slowly.

Temperature-programmed reduction. TPR of 50–100 mg of the samples was performed in a 5 vol% H_2-in-N_2 mixture (Air Liquide, ultrahigh-purity grade) at a flow rate of 25 ml min^{-1} using the thermal conductivity detector of a HP 5840 gas chromatograph to monitor the rate of hydrogen consumption. The temperature was increased from 323 to 873 K at the rate of 30 K min^{-1}.

Chemisorption measurements. Hydrogen chemisorption was measured in an all-glass system with PTFE valves, connected to an oil diffusion pump which was equipped with a liquid N_2 baffle and capable of evacuating the system to pressures lower than 10^{-2} Pa. Approximately 0.5 to 1 g of the prereduced catalyst was placed between two quartz wool plugs in a glass tube and reduced in flowing H_2 (100 ml min^{-1}) at 673 K for 2 h. Subsequently, the reactor was evacuated for 2 h at the same temperature.

Adsorption was carried out at 298 K and initial pressures between 4.9×10^4 and 6.9×10^4 Pa. Usually, the catalyst was permitted to equilibrate for 12 h at this pressure before the first hydrogen uptake was measured. The adsorption isotherms were obtained by subsequently decreasing the pressure and equilibrating for 1 h between all further data points. The total amount of adsorbed hydrogen extrapolated to zero pressure was used to calculate the dispersion.

X-ray diffraction measurements. Re-

duced samples were analyzed by means of a Siemens X-ray diffractometer using Cu$K\alpha$ radiation. The Scherrer equation was used to estimate the averaged particle size assuming spherical particles (*27*).

XPS measurements. All XPS spectra were recorded on a Surface Science Instrument SSX-100 spectrometer using monochromatized Al$K\alpha$ X rays. The spectrometer was calibrated against the Fermi edge of gold, and all binding energies were referenced to the Si 2*p* line at 103.0 eV. Typical instrument parameters of the analysis were a spot size of 600 μm and a pass energy of approximately 50 eV. Sample charging during XPS analysis was compensated by a flood gun operated at approximately 2 eV.

Magnetic measurements. Magnetization measurements were made for the Ni-containing catalysts using a Cahn Model 6602-4 Faraday apparatus capable of producing magnetic fields up to 10 kOe. The sample chamber was thermostated and could be purged with gas. Before measurements were made, samples of 5 mg were re-reduced for 2 h at 673 K *in situ*. Measurements of weight change versus magnetic field strength were made at both 77 and 300 K. Magnetization measurements at 77 K were extrapolated to infinite field strength to give values indicative of M_0 (saturation magnetization).

RESULTS

Temperature-Programmed Reduction

Variations in the reduction rates of the catalyst precursors during TPR are compiled in Fig. 1. The rate of reduction of the pure nickel catalyst exhibited a maximum at about 722 K. Upon addition of 10, 20, and 30 mol% Pt the maximum at 722 K did not appear. Instead, maxima of the reduction rate were observed at 653, 632, and 614 K, respectively. The intensity of the peaks decreased in the same sequence. In addition, a new peak with a maximum between 524 and 539 K appeared and increased in intensity with increasing concentration of Pt in the catalyst.

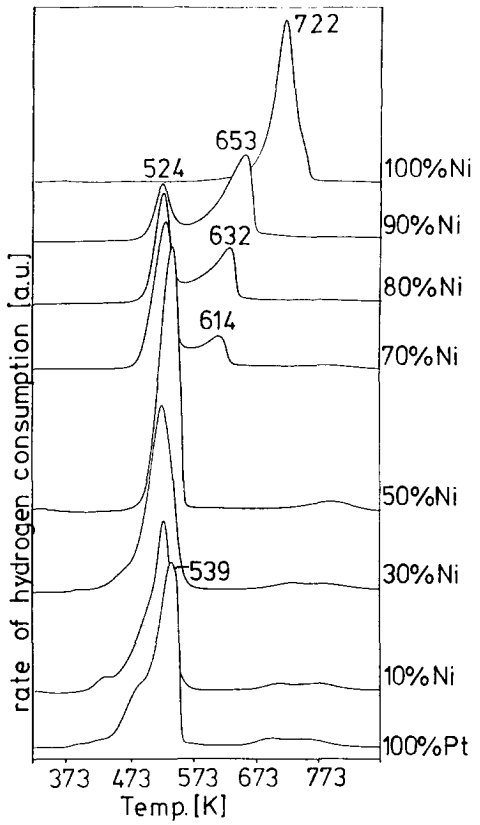

FIG. 1. Variations of the hydrogen consumption rates during TPR of silica-supported Ni/Pt catalysts.

Ni/Pt-4 (50 mol% Pt) had only one sharp maximum in the rate of reduction at 536 K. With Ni/Pt-5 and Ni/Pt-6 (70 and 90 mol% Pt), as well as with pure Pt, reduction behavior during TPR did not vary substantially compared to Ni/Pt-4. In contrast, the TPR of a physical mixture of $NiCl_2$ and $PtCl_4$ supported on silica, as well as of a mixture of unsupported $NiCl_2$ and $PtCl_4$, showed maxima in reduction rates similar to those of the single-component metals.

Chemisorption and Particle Size Distribution Measurements

Results from the hydrogen chemisorption measurements are compiled in Table 2. The average particle sizes determined from chemisorption measurements together with other estimates for particle size distribu-

TABLE 2

Hydrogen Chemisorption on Ni/SiO_2, Pt/SiO_2, and Ni/Pt Samples

	Ni (mol%)	H_2 adsorption ($\times 10^6$ mol/g)	Dispersion[a] (%)
Ni	100	31.8	15
Ni/Pt-1	90	32.0	16
Ni/Pt-2	80	39.4	20
Ni/Pt-3	70	39.3	20
Ni/Pt-4	50	37.1	19
Ni/Pt-5	30	25.6	13
Ni/Pt-6	10	31.6	16
Pt	0	44.2	22

[a] Based on total hydrogen uptake.

TABLE 3

Average Metal Particle Size of the Samples Investigated

	d_s(nm)[a]		d_v(nm)	
	Chemisorption	TEM	TEM	XRD
Ni	6.2	n.d.	n.d.	21.2
Ni/Pt-1	6.7	6.5	8.0	n.d.
Ni/Pt-2	5.8	n.d.	n.d.	n.d.
Ni/Pt-3	5.8	4.9	6.3	n.d.
Ni/Pt-4	6.2	4.6	5.7	9.1
Ni/Pt-5	9.5	6.9	8.0	n.d.
Ni/Pt-6	7.3	n.d.	n.d.	11.2
Pt	5.3	n.d.	n.d.	9.9

[a] d_s and d_v refer to surface- and volume-averaged particle size (*27, 28*).

tions are compiled in Table 3. To calculate the average particle sizes for the bimetallic catalysts from these data, catalyst surface compositions were assumed to be equal to the bulk compositions, and density and the number of surface atoms per square meter were adjusted according to the composition of the bimetallic phase.

Hydrogen chemisorption measurements show low dispersions in the range 16 to 27%, corresponding to particle sizes of 6.7 to 4.9 nm, respectively. Particle size distributions were obtained from TEM micrographs and are presented in Fig. 2. For each micrograph an average of 300 to 400 particles were counted and classified in five classes of particle size. For all catalysts,

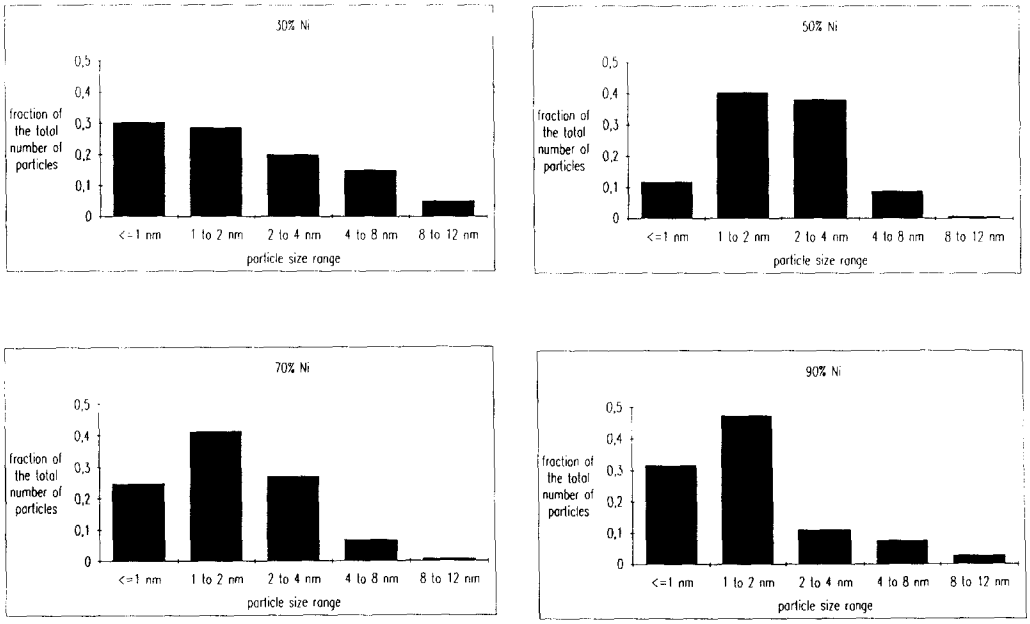

FIG. 2. Particle size distribution determined by means of transmission electron microscopy (bulk averaged).

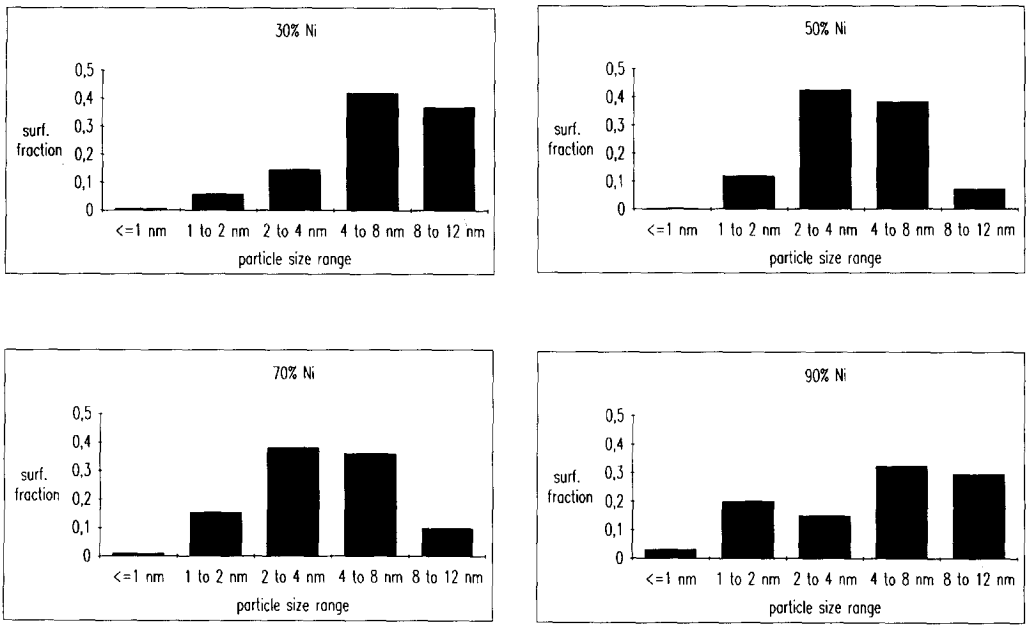

FIG. 3. Particle size distribution determined by means of transmission electron microscopy weighed by the contribution to accessible metal surface area.

the majority of the particles were smaller than 4 nm (see Fig. 2). On the other hand, when, the contributions of the various classes to the surface were compared, particles in the range 4 to 8 nm were much more dominant (Fig. 3). Agreement between surface-averaged particle sizes obtained from H_2 chemisorption and TEM was very good for Ni/Pt-1, whereas it was less satisfactory for the other samples. The presence of particles larger than 10 nm was observed for Ni/SiO_2. These large particles did not significantly contribute to the volume of hydrogen being adsorbed. In contrast, small Ni particles, which contain the majority of hydrogen adsorption sites, only weakly contributed to XRD and TEM signals.

X-ray Diffraction Measurements

The phases and crystallographic planes detected with XRD are compiled in Table 4. The presence of a bimetallic phase was detected for Ni/Pt-3, Ni/Pt-4, and Ni/Pt-5 (70, 50, and 30 mol% Ni). With Ni/Pt-5 and Ni/Pt-6, a pure platinum phase was detected. Similarly, samples Ni/Pt-1 and Ni/Pt-2 showed X-ray diffraction maxima of a pure Ni phase. The particle sizes were estimated from the integral peak width (*27*) and are compiled in Table 3.

XPS Measurements

After *in situ* reduction of the Ni/Pt samples, the binding energy of Pt $4f_{7/2}$ was found to be 70.5 ± 0.3 eV (referenced to Si $2p$ at 103.0 eV) for all samples. This binding

TABLE 4

Phases and Crystallographic Planes Detected with XRD

	Ni(111)	Ni(200)	NiPt(111)	NiPt(200)	Pt(111)	Pt(200)
Ni	*	*				
Ni/Pt-1	*					
Ni/Pt-2	*					
Ni/Pt-3			*			
Ni/Pt-4			*	*		
Ni/Pt-5			*	*	*	*
Ni/Pt-6					*	*
Pt					*	*

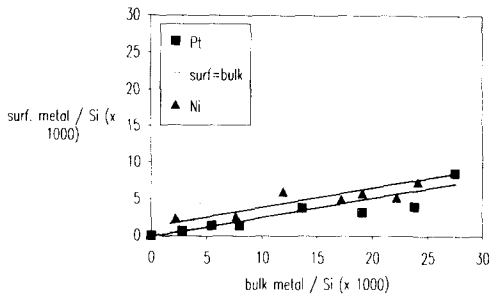

FIG. 4. "Surface" metal fraction versus bulk metal fraction of Ni and Pt of the silica-supported Ni/Pt samples.

energy is to be compared to that of bulk Pt at 71.1 eV. For catalysts containing more than 10% Ni, the binding energy for Ni $2p_{3/2}$ was 851.6 ± 0.2 eV, exactly that expected for bulk Ni metal. For the catalyst containing only 10% Ni, the binding energy of Ni $2p_{3/2}$ was 855.6 eV, suggesting the presence of unreducible Ni^{2+} at this lowest Ni loading.

Figure 4 shows a plot of the "surface" metal fraction, i.e., those metal atoms accessible for XPS analysis (Ni 2*p* or Pt 4*f* signal normalized to the Si 2*p* signal of the support) versus the number of bulk metal atoms per silicon atom of the support, for both Ni and Pt. In that graph, the points for Pt can be extrapolated to the origin. The slope of a straight line through the points for Pt is 0.2, equivalent to the approximately constant overall metal dispersion of 20% for all samples. Ni, on the other hand, has its first point (Ni/Pt-1) on the 45° line, indicating 100% dispersion of Ni at this lower concentration. A straight line through this and the other Ni points also exhibits a slope of 0.2 and is parallel to that for Pt, but is displaced by a constant amount.

Magnetic Measurements

An increase in weight was detected only for Ni, Ni/Pt-1, Ni/Pt-2, and Ni/Pt-3 samples. This quantity is related to the magnitude of magnetization. The relative magnetization did not change, indicating no change in the quality of the magnetic properties of Ni. The weight change normalized to the amount of Ni probed versus the fraction of Ni that is not alloyed or in close contact with Pt is plotted in Fig. 5. The magnitude of the observed effects for pure Ni suggests that Ni is in a superparamagnetic state, as is expected for small Ni particles supported on SiO_2 (*29*). Note that superparamagnetic behavior requires a larger ensemble of Ni atoms. Ni/Pt-1, Ni/Pt-2, and Ni/Pt-3 fall on a straight line which intercepts the abscissa at a value between 10 and 15% Ni. As the average particle size is fairly constant for the bimetallic

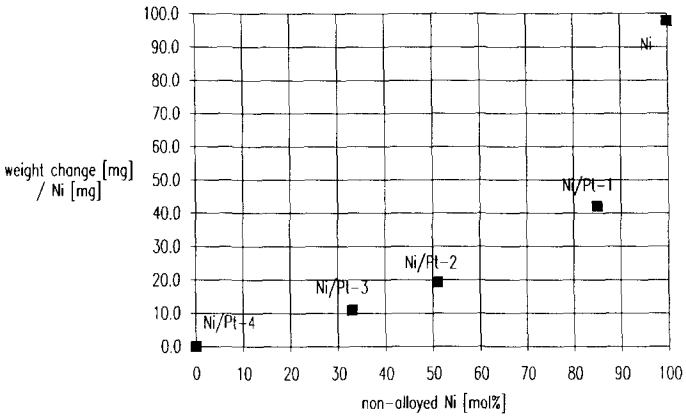

FIG. 5. Weight change normalized to the amount of Ni in the sample (indicating the magnetization) versus the amount of nonalloyed Ni estimated from TPR measurements.

samples, one expects that all free Ni particles contribute to the signal with the same intensity. The intercept between 10 and 15% Ni suggests that this fraction of the Ni atoms does not contribute to the signal. Because all other points are on a straight line we conclude that it is a constant fraction of 10 to 15% of Ni atoms which may be so highly dispersed at the surface that they are unable to exhibit superparamagnetic behavior. Note also that the 100% Ni catalyst showed a significantly higher magnetization than suggested by this correlation. This may be explained by the larger particle size found for the pure Ni catalyst.

DISCUSSION

Phase Composition

X-ray diffraction measurements suggest that a NiPt phase was formed in agreement with the phase diagram (*14*) for NiPt-3, -4, and -5 (70, 50, and 30% Ni). Ni_3Pt, a phase which is known to exist in the range 80 to 70% Ni, was not detected. A pure Pt phase was detected in Ni/Pt-5 and -6, and a pure Ni phase in Ni/Pt-1 and -2. The parallel presence of a NiPt phase and a separate Ni phase in Ni/Pt-3 (concluded from the TPR results) and of a Pt phase in Ni/Pt-5 suggests a heterogeneous distribution of the components. This heterogeneous distribution in return implies the absence of a homogeneous solid solution of Pt and Ni between concentrations of 30 and 70% Pt (Ni) in bimetallic catalysts. Because only the NiPt phase was detected with Ni/Pt-4 (50% Ni), we conclude that the presence of two phases in Ni/Pt-3 and Ni/Pt-5 is not due to our preparation procedure. The rather broad diffraction lines for the NiPt phase was concluded to be due to the small size of the alloy particles. In agreement with other studies (*20, 26*), interatomic distances calculated from the lattice parameters do not follow Vegard's law, which predicts a linear correlation between alloy composition and interatomic distance. This is, however, not unusual because the NiPt forms a separate phase and not a solid solution of Ni in Pt or vice versa.

It is interesting to note that the NiPt phase was formed immediately after the maximum in the rate of reduction as seen by XRD. Thus, we conclude that increasing the reduction temperature increases the size of the alloy particles but is not crucial to formation of the alloy.

Kinetics of Reduction

The TPR profiles (Fig. 1) show that supported nickel chloride and platinum chloride have maxima in the rate of reduction at 722 and 539 K. Thus, for pure phases, reduction of the platinum salt was concluded to be completed before reduction of the nickel salt starts.

Addition of Pt to Ni had two effects: (i) A new reduction maximum appeared at 524 K [low-temperature (LT) peak]. (ii) The maximum in the rate of reduction at 722 K [high-temperature (HT) peak] in Ni/SiO_2 was gradually shifted to lower temperatures. Both effects are clearly affiliated with the presence of Pt. The intensity of the maximum at lower temperatures increased with platinum concentration, and the temperature of the maximum of the HT peak decreased as the platinum content increased.

Because of the similarity with the reduction behavior of Ni, we attribute the HT peak to reduction of a more or less pure Ni precursor phase. The rate of reduction of these cations is increased and the temperature of the maximum is decreased by the presence of a metallic phase (Pt or NiPt alloy) during the temperature interval of the HT reduction peak and thus by the presence of spilt-over hydrogen dissociated on the metallic phase. This is in qualitative agreement with earlier investigations by Geus *et al.* (*26*). Note that the physical mixture of chloride precursors of Pt/SiO_2 and Ni/SiO_2 did not lead to a similar phenomenon. Thus, we conclude that the distance between reduced and unreduced particles must be very small to exert a significant effect on reduction kinetics. This view is

supported by the gradual decrease in the temperature for the maximum reduction rate of $NiCl_2$ (HT peak). With increasing concentration of the reduced particles (PtNi), the average probable distance between a reduced metal particle and an unreduced Ni salt particle decreases.

Quantitative evaluation of the TPR peaks reveals almost 100% apparent degree of reduction for the nickel precursor and about 77% apparent degree of reduction (amount of hydrogen detected for one reduction peak divided by amount of hydrogen necessary for complete reduction of the metal salts × 100) for the platinum precursor. This implies either (i) that the platinum precursor was not completely reduced or (ii) that partial reduction already occurred between 298 and 323 K during stabilization of the TCD detector. The second possibility seems more plausible to us, because the rate of reduction of $PtCl_4$ reaches a maximum value about 200 K below that of $NiCl_2$. Moreover, Hoyle *et al.* (*30*) reported the appearance of a maximum in the rate of reduction of Pt below ambient temperature. The contribution of this peak to overall hydrogen consumption was found to be in the range 5 to 50% depending mainly on the total loading and the method of preparation, i.e., impregnation or ion exchange. Considering these results, we conclude for the Pt/SiO_2 catalyst that part of the precursor salt was already reduced before the start of the TPR experiments.

Assuming that the 100% apparent reducibility of Ni/SiO_2 does not change in the bimetallic samples, 85, 51, and 33% of the Ni in Ni/Pt-1, Ni/Pt-2, and Ni/Pt-3, respectively, are reduced during the HT maximum of the TPR experiment and are, thus, present as separate Ni phase. In return, that amount determines the concentration of the phase (or intimate mixture) that is reduced in the LT peak.

Although it is straightforward that the LT maximum of the TPR is affiliated with reduction of a Pt-rich phase, the exact nature of this phase (mixture) is difficult to assess directly for samples with a low concentration of platinum. XRD results only confirm the presence of a stoichiometric PtNi phase for the sample containing 30% Pt. If we assume that a stoichiometric compound NiPt is formed upon addition of Pt to the supported Ni catalyst, we would expect to find 88, 75, and 57% of the Ni in separate Ni phases. Because the values expected according to this model are higher than those determined by TPR in all cases, we conclude that either a stoichiometric Ni_3Pt compound must be present in concentrations decreasing with increasing concentration of Pt or a solid solution of both metals exists. The phase diagram suggests that both possibilities are feasible (*14*). With Ni/Pt-4, only the presence of stoichiometric NiPt was observed, which showed reduction behavior during TPR very similar to that of pure Pt. Thus, we conclude that the presence of a significant fraction of Pt suffices to reproduce the reduction kinetics of pure Pt.

Semiquantitative analysis of XPS and magnetic measurements suggests the presence of a highly dispersed fraction of Ni (10–15%) which may be present in all the Ni-containing samples. We speculate that this fraction of Ni strongly interacts with the support and forms a mixed oxide phase in the oxidized state.

CONCLUSIONS

Formation of Ni/Pt alloys in Ni/Pt bimetallic catalyst was found to take place and to be quantitative with respect to the less abundant constituent. For all samples, with the exception of Ni/Pt-4 (50 mol% Pt), the pure metal phase of the more abundant constituent was detected. Thus, we conclude that solid solutions were formed only in a limited concentration region as suggested by the phase diagram (*14*). During TPR, the presence of metallic Pt and PtNi alloys facilitates the reduction of Ni. This is manifested by the appearance of the TPR peak at low temperature (increasing in intensity with increasing Pt concentration) and the

decrease in size and temperature of the HT peak.

ACKNOWLEDGMENTS

This work was supported by the Fonds zur Förderung der Wissenschaftlichen Forschung under project P6912 CHE and by the U.S. Department of Energy and Office of Basic Energy Science. Helpful discussions with G. Hilscher and P. Mohn are gratefully acknowledged.

REFERENCES

1. Thomas, Ch. L., "Catalytic Processes and Proven Catalysts." Academic Press, New York/London, 1970.
2. Nowak, E. J., and Koros, R. M., *J. Catal.* **7,** 50 (1967).
3. van't Blik, H. F., and Prins, R., *J. Catal.* **97,** 188 (1986).
4. Martens, J. H. A., van't Blik, H. F., and Prins, R., *J. Catal.* **97,** 200 (1986).
5. van't Blik, H. F., Konigsberger, D. C., and Prins, R., *J. Catal.* **97,** 210 (1986).
6. van Hook, J. P., *Catal. Rev.-Sci. Eng.* **21,** 1 (1980).
7. Heinemann, H., *in* "Catalysis, Science and Technology" (J. R. Anderson and M. Boudart, Eds.), Vol. 1, p. 1. Springer-Verlag, Berlin/Heidelberg/New York, 1981.
8. Prasad, R., Kennedy, L. A., and Ruckenstein, E., *Catal. Rev.-Sci. Eng.* **26,** 1 (1984).
9. Sinfelt, J. H., *in* "Catalysis, Science and Technology" (J. R. Anderson and M. Boudart, Eds.), Vol. 1, p. 257. Springer-Verlag, Berlin/Heidelberg/New York, 1981.
10. Sinfelt, J. H., *Catal. Rev.-Sci. Eng.* **3,** 175 (1970).
11. Tanaka, K., *Stud. Surf. Sci. Catal.* **27,** 79 (1986).
12. Vannice, M. A., *J. Catal.* **50,** 228 (1977).
13. Bertolini, J. C., Tardi, B., Abon, M., Billy, J., Delichere, P., and Massardier, J., *Surf. Sci.* **135,** 117 (1983).
14. Hansen, M., Anderko, K., "Constitution of Binary Alloys," p. 1032. McGraw–Hill, New York, 1958.
15. Gauthier, Y., Baudoing, R., Joly, Y., Rundgren, J., Bertolini, J. C., and Massardier, J., *Surf. Sci.* **162,** 342 (1985).
16. Burton, J. J., and Polizzotti, R. S., *Surf. Sci.* **66,** 1 (1977).
17. Spencer, M. S., *Surf. Sci.* **145,** 153 (1984).
18. Sedlacek, J., Hilaire, L., Legare, P., and Maire, G., *Surf. Sci.* **115,** 541 (1982).
19. Dominguez, J. M., Vasquez, A. S., Renouprez, A. J., and Yacaman, M. J., *J. Catal.* **75,** 101 (1982).
20. Bommanavar, A. S., Montano, P. A., and Yacaman, M. J., *Surf. Sci.* **156,** 426 (1985).
21. Renouprez, A. J., Morawek, B., Imelik, B., Perrichon, V., Domingez-Esquivel, J. M., and Jablonski, J., *Stud. Surf. Sci. Catal.* **7,** 173 (1980).
22. Sachtler, W. M. H., and van Santen, R. A., *Appl. Surf. Sci.* **3,** 121 (1979).
23. de Temmermann, L., Creemers, C., van Hove, H., and Neyens, A., *Surf. Sci.* **183,** 565 (1987).
24. de Temmermann, L., Cremers, C., van Hove, H., Neyens, A., Bertolini, J. C., and Massardier, J., *Surf. Sci.* **178,** 888 (1986).
25. Wielers, A. F. H., Dings, M. M. M., van der Grift, C. J. G., and Geus, J. W., *Appl. Catal.* **24,** 299 (1986).
26. van Stiphout, P. C. M. and Geus, J. W., *Appl. Catal.* **25,** 19 (1986).
27. Lemaitre, J. L., Menon, P. G., and Delannay, F., *in* "Characterization of Heterogeneous Catalysts" (F. Delannay, Ed.), p. 299. Marcel Dekker, New York, 1984.
28. Shastri, A. G., Schwank, J., and Galvagno, S., *J. Catal.* **100,** 446 (1986).
29. Dreyer, H., *Z. Anorg. Allg. Chem.* **362,** 233 (1968).
30. Hoyle, N. D., Newbatt, P. H., Rollins, K., Sermon, P. A., and Wurie, A. T., *J. Chem. Soc. Faraday Trans. 1* **81,** 2605 (1985).